

## Existence of the Halocarbonyl and Trifluoromethyl Cations in the Condensed Phase

K. O. Christe,<sup>\*,†,‡</sup> B. Hoge,<sup>†,§</sup> J. A. Boatz,<sup>‡</sup> G. K. S. Prakash,<sup>†</sup> G. A. Olah,<sup>†</sup> and J. A. Sheehy<sup>‡</sup>

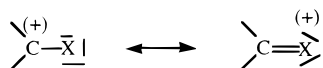
Loker Hydrocarbon Research Institute, University of Southern California, Los Angeles, California 90089 and Air Force Research Laboratory, Edwards AFB, California 93524

Received March 11, 1999

Experimental and theoretical studies show that neither  $\text{CF}_3^+$  nor  $\text{FCO}^+$  can be stabilized in the condensed phase with presently known Lewis acids. In the case of  $\text{ClCO}^+$ , stabilization with  $\text{SbF}_6^-$  was also not possible, but  $\text{Sb}_3\text{F}_{15}$  possesses sufficient acidity to abstract a fluoride ion from  $\text{ClFCO}$  in the formation of  $\text{ClCO}^+\text{Sb}_3\text{F}_{16}^-$ . This salt was fully characterized, providing the first well-established proof for the existence of a halocarbonyl cation in the condensed phase. Theoretical calculations and thermochemical cycles were used to corroborate our experimental findings, demonstrating that it is possible to predict correctly whether a molecule with three different donor sites, such as  $\text{ClFCO}$ , will form an oxygen-coordinated donor–acceptor adduct or undergo either  $\text{F}^-$  or  $\text{Cl}^-$  abstraction. Furthermore, a method is described for extending natural bond orbital (NBO) analyses to systems containing two different types of competing,  $p(\pi)$  back-donating ligands.

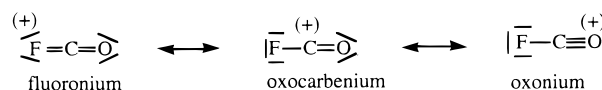
## Introduction

Carbocations play an important role as reactive intermediates in organic synthesis.<sup>1–3</sup> In tricoordinate carbenium ions, the carbon center is usually stabilized by back-donation of a free valence electron pair from a ligand X, which in a simple valence bond description shifts some of the formal positive charge from carbon to the ligand. With increasing electronegativity, however,

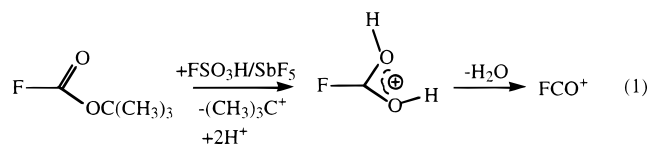


the ligand increasingly resists this electron transfer.<sup>4</sup> Consequently, it is not surprising that condensed phase  $\text{CF}_3^+$  is still unknown, although the free cation is vibrationally stable<sup>4</sup> and has been observed by electron impact studies in the gas phase,<sup>5</sup> whereas the heavier halogen analogues, i.e.,  $\text{CCl}_3^+$ ,  $\text{CBr}_3^+$ , and  $\text{CI}_3^+$ , have been characterized in solution by NMR spectroscopy.<sup>6</sup>

A closely related and challenging problem is the condensed state preparation of  $\text{FCO}^+$ . In this cation, two of the fluorine ligands have been replaced by an oxygen atom, which although highly electronegative, should be a better  $p(\pi)$  back-donor than fluorine, as shown by the following valence bond structures.



The free  $\text{FCO}^+$  cation is also vibrationally stable and has previously been characterized by microwave spectroscopy in a liquid nitrogen cooled, negative glow discharge.<sup>7</sup> Furthermore, its heavier halogen analogues,  $\text{ClCO}^+$ ,  $\text{BrCO}^+$ , and  $\text{ICO}^+$ , have been observed in  $\text{SO}_2\text{ClF}$  solution by  $^{13}\text{C}$  NMR spectroscopy, but attempts have failed to detect  $\text{FCO}^+$  using similar approaches.<sup>8</sup> Very recently, however, a minor  $^{13}\text{C}$  NMR signal, observed at  $-78^\circ\text{C}$  in the protolytic ionization of *tert*-butyl fluoroformate with a 5-fold excess of  $\text{FSO}_3\text{H}/\text{SbF}_5$ , was attributed to  $\text{FCO}^+$ .<sup>9</sup> It was suggested to have been formed by dehydration of protonated fluoroformic acid (eq 1), whose formation was firmly established by  $^{13}\text{C}$ ,  $^1\text{H}$ , and  $^{19}\text{F}$  NMR spectroscopy.<sup>9</sup>



Since the reported<sup>8,9</sup> experimental evidence for the existence of  $\text{FCO}^+$  and  $\text{ClCO}^+$  in the condensed state rested exclusively on the observation of  $^{13}\text{C}$  NMR signals in the vicinity of the predicted shift ranges, and  $\text{F}_2\text{CO}$  and  $\text{Cl}_2\text{CO}$  are well-known to form the stable oxygen-bridged, donor–acceptor adducts  $\text{F}_2\text{CO}\cdot\text{AsF}_5$ ,  $\text{F}_2\text{CO}\cdot\text{SbF}_5$ ,<sup>10</sup> and  $\text{Cl}_2\text{CO}\cdot\text{AlCl}_3$ ,<sup>11</sup> it was important to reexamine the experimental evidence for the existence of

<sup>†</sup> Loker Hydrocarbon Research Institute.<sup>‡</sup> Air Force Research Laboratory.<sup>§</sup> Present address: Institute of Inorganic Chemistry, University of Cologne, Germany.

- (1) Olah, G. A. *Friedel–Crafts Chemistry*; Wiley: New York, 1973.
- (2) Olah, G. A. *Carbocations and Electrophilic Reactions*; Wiley: New York, 1973.
- (3) *Stable Carbocation Chemistry*; Prakash, G. K. S., Schleyer, P. v. R., Eds.; Wiley: New York, 1997.
- (4) Frenking, G.; Fau, S.; Marchand, C. M.; Grützmacher, H. *J. Am. Chem. Soc.* **1997**, *119*, 6648.
- (5) Martin, R. H.; Lampe, F. W.; Taft, R. W. *J. Am. Chem. Soc.* **1966**, *88*, 1353.
- (6) Olah, G. A.; Rasul, G.; Heiliger, L.; Prakash, G. K. S. *J. Am. Chem. Soc.* **1996**, *118*, 3580. Olah, G. A.; Heiliger, L.; Prakash, G. K. S. *J. Am. Chem. Soc.* **1989**, *111*, 8020.

- (7) Botschwina, P.; Sebal, P.; Bogey, M.; Demuyne, C.; Destombes, J.-L. *J. Mol. Spectrosc.* **1992**, *153*, 255.
- (8) Prakash, G. K. S.; Bausch, J. W.; Olah, G. A. *J. Am. Chem. Soc.* **1991**, *113*, 3203.
- (9) (a) Olah, G. A.; Burrichter, A.; Mathew, T.; Vankar, Y. D.; Rasul, G.; Prakash, G. K. S. *Angew. Chem., Int. Ed. Engl.* **1997**, *36*, 1875. (b) Sorensen, T. S. *Angew. Chem., Int. Ed.* **1998**, *37*, 603.
- (10) Chen, G. S. H.; Passmore, J. J. *J. Chem. Soc., Dalton Trans.* **1979**, 1257.
- (11) Christe, K. O. *Inorg. Chem.* **1967**, *6*, 1706.

FCO<sup>+</sup> and ClCO<sup>+</sup> in the condensed phase. Furthermore, it was interesting to explore under which conditions the oxygen-bridged donor-acceptor adducts and the ionic halocarbonyl salts can be formed and to evaluate the relative contributions of the halogens and oxygen to the electron back-donation in the corresponding carbocations. Another point of interest was the relative donor strength of fluorine, chlorine, and oxygen toward strong Lewis acids. Partial results from this study have been presented at two meetings,<sup>12</sup> and a full account is given in this paper.

### Experimental Section

**Materials and Apparatus.** Commercially available phosgene (Matheson), F<sub>2</sub>CO (PCR Research Chemicals), AsF<sub>5</sub>, and SbF<sub>5</sub> (Ozark Mahoning) were purified by fractional condensation prior to use. Literature methods were used for the syntheses of ClFCO,<sup>13</sup> Cl<sub>2</sub>CO·SbF<sub>5</sub>,<sup>14</sup> and *tert*-butyl fluoroformate.<sup>15</sup>

Volatile materials were handled in a stainless steel vacuum line equipped with Teflon-FEP U-traps, stainless steel bellows-seal valves, and a Heise Bourdon tube-type pressure gauge.<sup>16</sup> The line and other hardware were passivated with ClF<sub>3</sub> and HF. Nonvolatile materials were handled in the dry nitrogen atmosphere of a glovebox.

**Vibrational Spectra.** Raman spectra were recorded on a Cary Model 83GT with the 488 nm exciting line of a Lexel model 95 Ar-ion laser, using sealed glass tubes as sample containers. A previously described device<sup>17</sup> was used for recording the low-temperature spectra. Infrared spectra were recorded in the range of 4000–300 cm<sup>-1</sup> on a Midac model M FTIR spectrometer. For the low-temperature spectra, the cold sample was placed inside the glovebox between cold AgCl windows, which were mounted in a liquid N<sub>2</sub>-cooled copper block, mated with an O-ring flange to an evacuable glass cell with outer CsI windows.

**Nuclear Magnetic Resonance Spectroscopy.** The NMR spectra were recorded on a Varian Unity 300 MHz NMR spectrometer equipped with a 5 mm variable-temperature broad band probe. Sealed capillaries, which were filled with acetone-*d*<sub>6</sub> as lock substance, TMS as <sup>13</sup>C reference, and CFCl<sub>3</sub> or C<sub>6</sub>H<sub>5</sub>CF<sub>3</sub> as <sup>19</sup>F reference, were placed inside the NMR tubes.

**Preparation of [ClCO][Sb<sub>3</sub>F<sub>16</sub>].** On the vacuum line, ClFCO (3.2 mmol) was condensed at -196 °C into a 3/4 in. o.d. Teflon-FEP ampule, which was closed by a steel valve and contained a weighed amount (9.5 mmol) of SbF<sub>5</sub> dissolved in 4 mL of SO<sub>2</sub>ClF. The reaction mixture was stirred with a Teflon-coated magnetic stirring bar for 1 h at -78 °C. After the clear colorless solution was warmed to -64 °C (CHCl<sub>3</sub> slush bath), the gas phase above the liquid did not contain any ClFCO and F<sub>2</sub>CO, as shown by infrared spectroscopy. The solvent was pumped off overnight at -64 °C. The resulting white powder consisted of [ClCO][Sb<sub>3</sub>F<sub>16</sub>] (2.323 g, 3.15 mmol).

**NMR Spectroscopic Characterization of [ClCO][*cis*-Sb<sub>3</sub>F<sub>16</sub>].** A solution of ClFCO and 3 equiv of SbF<sub>5</sub> in SO<sub>2</sub>ClF at -60 °C showed only the previously reported<sup>8</sup> <sup>13</sup>C NMR signal (singlet at 134 ppm) for the ClCO<sup>+</sup> cation. The <sup>19</sup>F NMR spectrum exhibited broad multiplets in the Sb-F region from -90 to -140 ppm, characteristic for *cis*-Sb<sub>3</sub>F<sub>16</sub>.<sup>18</sup>

Under similar conditions, a 1:2 mixture of ClFCO and SbF<sub>5</sub> resulted in two <sup>13</sup>C NMR signals: a doublet at 164 ppm (<sup>1</sup>J(CF) 383 Hz) for the ClFCO-SbF<sub>5</sub> adduct<sup>14</sup> and a singlet at 134 ppm for the ClCO<sup>+</sup> cation. The corresponding <sup>19</sup>F NMR spectrum showed sharp signals (-141.0, -127.7, -112.2, -108.3, and -89.5 ppm) with the coupling

pattern characteristic of the *cis*-Sb<sub>3</sub>F<sub>16</sub><sup>-</sup> anion (-141.1, -127.8, -112.4, -108.3, -89.7)<sup>18</sup> and the relative intensities of 2.5:1.8:7.5:2.2:2. The <sup>19</sup>F NMR spectrum also showed two doublets, a more intense one at -109.6 and a less intense one at -105.2 ppm, which are characteristic of the four equivalent fluorine atoms in the 1:1 complexes, ClFCO·SbF<sub>5</sub> and SO<sub>2</sub>ClF·SbF<sub>5</sub>, respectively (literature values: -110.0 and -105.1 ppm, respectively).<sup>19</sup> The quintet resonances, expected for the single axial fluorine atoms of these compounds, were not observed. The <sup>19</sup>F resonance, due to the fluorine atom of the ClFCO part of the ClFCO·SbF<sub>5</sub> adduct, was observed at 74 ppm. The value of 59.9 ppm, previously reported<sup>19</sup> for this resonance, is incorrect and is due to free ClFCO.<sup>20</sup>

**Protolytic Ionization of *tert*-Butyl Fluoroformate.** *tert*-Butyl fluoroformate was added at -196 °C to a frozen, 1 molar solution of a 5-fold excess of FSO<sub>3</sub>H/SbF<sub>5</sub> (1/1 mole ratio) in SO<sub>2</sub>ClF and warmed to -78 °C. After the NMR spectra of the intensely yellow solution were recorded at -78 °C, the sample was allowed to warm to room temperature for about 10 min, and the spectra were rerecorded at -78 °C. No signs for either decomposition or any other changes were observed. The spectra exhibited only the previously reported resonances due to protonated fluoroformic acid and the *tert*-butyl cation,<sup>9</sup> except for the missing minor doublet signal at δ 117.5 in the <sup>13</sup>C spectrum.

**Computational Methods.** Vibrational spectra for FCO<sup>+</sup> and ClCO<sup>+</sup>, as well as the isoelectronic and well-known species FCN and ClCN, were computed using the single- and double-excitation coupled-cluster method<sup>21</sup> with a noniterative treatment of connected triple excitations, denoted CCSD(T),<sup>22</sup> in 6-311+G(2d) atomic basis sets.<sup>23</sup> At the CCSD(T) geometries, isotropic nuclear magnetic resonance shieldings were computed using the GIAO-MBPT(2) approach,<sup>24</sup> which employs the gauge-including atomic orbital (GIAO) solution to the gauge-invariance problem<sup>25</sup> and density matrixes obtained from second-order many-body perturbation theory [MBPT(2)]. The ACES II program systems<sup>26</sup> on IBM RS/6000 work stations were used for these calculations.

Natural bond orbital (NBO) analyses<sup>27</sup> of the one-electron density matrixes obtained from single- and double-excitation quadratic configuration-interaction (QCISD) calculations<sup>28</sup> were carried out for FCO<sup>+</sup> and ClCO<sup>+</sup>, as well as for a series of benchmark compounds that included FCN, ClCN, CF<sub>3</sub><sup>+</sup>, CCl<sub>3</sub><sup>+</sup>, BF<sub>3</sub>, and BCl<sub>3</sub>. In this approach, the molecular wave function is decomposed through a set of natural bond orbitals into localized bonding, antibonding, and lone-pair units. These computations were carried out using the Gaussian 94 program system.<sup>29</sup>

Constrained geometry optimizations of SbF<sub>5</sub> + ClFCO and Sb<sub>3</sub>F<sub>15</sub> + ClFCO were performed using density functional methods. The

- (12) (a) Christe, K. O.; Hoge, B.; Sheehy, J.; Wilson, W.; Zhang, X. NF<sub>4</sub><sup>+</sup> and Carbocation Chemistry. Paper 036 presented in the Division of Fluorine Chemistry at the 216th ACS National Meeting, Boston, MA, August 23–27, 1998. (b) Hoge, B.; Sheehy, J. A.; Prakash, G. K. S.; Olah, G. A.; Christe, K. O. On the Existence of the Halocarbonyl Cations. Paper B39 presented at the 12th European Symposium on Fluorine Chemistry, Berlin, Germany, August 29–September 2, 1998.
- (13) Hoge, B.; Boatz, J. A.; Christe, K. O. *Inorg. Chem.*, in press.
- (14) Hoge, B.; Christe, K. O. *J. Fluor. Chem.* **1999**, *94*, 107.
- (15) Wackerle, L.; Ugi, I. *Synthesis* **1975**, 598.
- (16) Christe, K. O.; Wilson, R. D.; Schack, C. J. *Inorg. Synth.* **1986**, *24*, 3.
- (17) Miller, F. A.; Harney, B. M. *Appl. Spectrosc.* **1969**, *23*, 8.
- (18) Bacon, J.; Dean, P. A. W.; Gillespie, R. J. *Can. J. Chem.* **1970**, *48*, 3413.

- (19) Bacon, J.; Dean, P. A. W.; Gillespie, R. J. *Can. J. Chem.* **1971**, *49*, 1276.
- (20) Schaumburg, K. J. *Magn. Reson.* **1972**, *7*, 177.
- (21) Purvis, G. D., III; Bartlett, R. J. *J. Chem. Phys.* **1982**, *76*, 1910.
- (22) Raghavachari, K.; Trucks, G. W.; Pople, J. A.; Head-Gordon, M. *Chem. Phys. Lett.* **1989**, *157*, 479.
- (23) Frisch, M. J.; Pople, J. A.; Binkley, J. S. *J. Chem. Phys.* **1984**, *80*, 3265.
- (24) Gauss, J. *Chem. Phys. Lett.* **1992**, *191*, 614.
- (25) Ditchfield, R. *Mol. Phys.* **1974**, *27*, 789.
- (26) Stanton, J. F.; Gauss, J.; Watts, J. D.; Nooijen, M.; Oliphant, N.; Perera, S. A.; Szalay, P. G.; Lauderdale, W. J.; Gwaltney, S. R.; Beck, S.; Balkova, A.; Bernholdt, D. E.; Baeck, K.-K.; Rozyczko, P.; Sekino, H.; Hober, C.; Bartlett, R. J. ACES II, Quantum Theory Project; University of Florida, Gainesville, FL, 1992. Integral packages included are VMOL (Almlöf, J.; Taylor, P. R.), BPROPS (Taylor, P. R.), and ABACUS (Helgaker, T.; Jensen, H. J. Aa.; Jorgensen, P.; Olsen, J.; Taylor, P. R.).
- (27) Reed, A. E.; Curtiss, L. A.; Weinhold, F. *Chem. Rev.* **1988**, *88*, 1899.
- (28) Pople, J. A.; Head-Gordon, M.; Raghavachari, K. *J. Chem. Phys.* **1987**, *87*, 5968.
- (29) (a) Frisch, M. J.; Trucks, G. W.; Schlegel, H. B.; Gill, P. M. W.; Johnson, B. G.; Robb, M. A.; Cheeseman, J. R.; Keith, T.; Peterson, G. A.; Montgomery, J. A.; Raghavachari, K.; Al-Laham, M. A.; Zakrzewski, V. G.; Ortiz, J. V.; Foresman, J. B.; Cioslowski, J.; Stefanov, B. B.; Nanayakkara, A.; Challacombe, M.; Peng, C. Y.; Ayala, P. Y.; Chen, W.; Wong, M. W.; Andres, J. L.; Replogle, E. S.; Gomperts, R.; Martin, R. L.; Fox, D. J.; Binkley, J. S.; Defrees, D. J.; Baker, J.; Stewart, J. P.; Head-Gordon, M.; Gonzalez, C.; Pople, J. A. *Gaussian 94*, Revision E. 2; Gaussian, Inc.: Pittsburgh, PA, 1995. (b) Glendening, E. D.; Reed, A. E.; Carpenter, J. E.; Weinhold, F. NBO, Version 3.1; University of Wisconsin: Madison, WI, 1987.

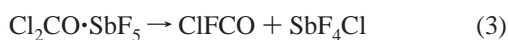
B3LYP hybrid functional<sup>30</sup> and the Stevens, Basch, Krauss, Jasien, and Cundari effective core potentials and the corresponding valence double- $\zeta$  basis sets<sup>31</sup> were used. The basis set was augmented with a diffuse s+p shell<sup>32</sup> and a single Cartesian d polarization function on each atom.<sup>33</sup> These calculations, hereafter denoted as B3LYP/SBK+(d), were also performed using Gaussian 94.<sup>29</sup>

## Results and Discussion

**Cl<sub>2</sub>CO/MF<sub>5</sub> (M = As, Sb) Systems.** By analogy with AlCl<sub>3</sub>,<sup>11</sup> the pnictogen pentafluorides, AsF<sub>5</sub> and SbF<sub>5</sub>, form with Cl<sub>2</sub>CO exclusively, O-coordinated, 1:1 donor–acceptor adducts (eq 2). A detailed investigation of these adducts is given



elsewhere.<sup>13</sup> On thermal decomposition of the solid Cl<sub>2</sub>CO·SbF<sub>5</sub> adduct or in SO<sub>2</sub>ClF solution at –78 °C, a quantitative chlorine–fluorine exchange of one of the two chlorine ligands of Cl<sub>2</sub>CO was observed (eq 3).<sup>14</sup>



**F<sub>2</sub>CO/MF<sub>5</sub> (M = As, Sb) Systems.** By analogy with Cl<sub>2</sub>CO and in accord with a previous report,<sup>10</sup> F<sub>2</sub>CO and SbF<sub>5</sub> or AsF<sub>5</sub> form exclusively O-coordinated, donor–acceptor adducts (eq 4).<sup>13</sup>



There was no evidence for the formation of ionic FCO<sup>+</sup> salts, either at low temperature in SO<sub>2</sub>ClF solution or when a large excess of SbF<sub>5</sub> was used either as a solvent for the enhancement of the Lewis acidity or as a matrix.

**ClFCO/MF<sub>5</sub> (M = As, Sb) Systems.** With AsF<sub>5</sub> at any mole ratio or SbF<sub>5</sub> at a 1:1 mole ratio, ClFCO forms exclusively, O-coordinated, 1:1 donor–acceptor adducts (eq 5).<sup>13</sup>



With a 2-fold excess of SbF<sub>5</sub>, however, ClFCO forms in SO<sub>2</sub>-ClF solution the ionic ClCO<sup>+</sup>Sb<sub>3</sub>F<sub>16</sub><sup>–</sup> salt (eq 6), as observed earlier.<sup>8</sup>



With a smaller excess of SbF<sub>5</sub>, both the ClCO<sup>+</sup>Sb<sub>3</sub>F<sub>16</sub><sup>–</sup> salt and the ClFCO·SbF<sub>5</sub> adduct were observed in the low-temperature NMR spectra of the SO<sub>2</sub>ClF solutions. However, when these solutions were pumped to dryness at –20 °C, the solid residue consisted exclusively of ClCO<sup>+</sup>Sb<sub>3</sub>F<sub>16</sub><sup>–</sup>, and the observed material balance corresponded to the uptake of 1 mol of ClFCO per 3 mol of SbF<sub>5</sub>. When a larger than 2-fold excess of SbF<sub>5</sub> was used in these reactions, the extra SbF<sub>5</sub> formed with the SO<sub>2</sub>ClF solvent the well-known<sup>18,34</sup> SO<sub>2</sub>ClF·SbF<sub>5</sub> adduct, and

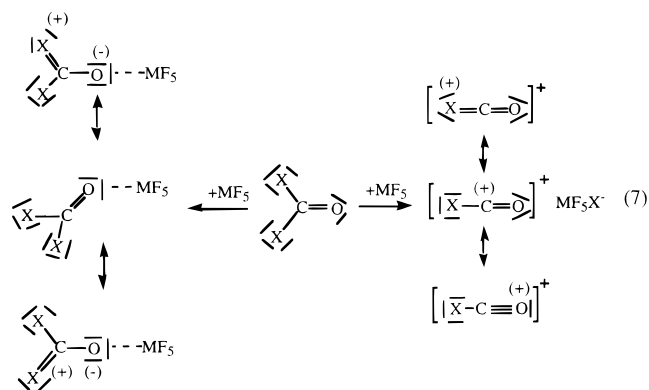
no polyantimonates, containing more than three antimony atoms, were observed.

These results demonstrate that neither monomeric SbF<sub>5</sub> nor many AsF<sub>5</sub> molecules are sufficiently acidic to abstract a fluoride ion from ClFCO, and that at least three SbF<sub>5</sub> molecules are required to accomplish this task. For acidities lower than that of (SbF<sub>5</sub>)<sub>3</sub>, O-coordinated, donor–acceptor adducts are formed.

Since the above findings for the F<sub>2</sub>CO/MF<sub>5</sub> systems could not be reconciled with the previous claim<sup>9</sup> for the existence of FCO<sup>+</sup> under essentially identical conditions, i.e., SO<sub>2</sub>ClF solutions at subambient temperature with SbF<sub>6</sub><sup>–</sup>·nSbF<sub>5</sub> as a counterion, the previously published<sup>9</sup> protolytic ionization of *tert*-butyl fluoroformate with a 5-fold excess of FSO<sub>3</sub>H/SbF<sub>5</sub> was repeated. In several attempts by different coauthors of this paper, the <sup>13</sup>C NMR signal, observed at 117.5 ppm and attributed to FCO<sup>+</sup>,<sup>9</sup> could not be reproduced. Therefore, the previous claim<sup>9</sup> for the observation of FCO<sup>+</sup> in the condensed phase may be incorrect, while that<sup>8</sup> for ClCO<sup>+</sup> is confirmed by both NMR and vibrational spectroscopy (see below). It should be noted that the <sup>13</sup>C NMR shift (117.5 ppm) and coupling constant (*J*<sub>C,F</sub> = 322 Hz), previously attributed<sup>9</sup> to FCO<sup>+</sup>, are very close to those measured for CFCI<sub>3</sub> ( $\delta$  117.8 and *J*<sub>C,F</sub> = 335 Hz as a 3 M solution in CD<sub>3</sub>COCD<sub>3</sub>), which might have been formed accidentally as a byproduct in the original experiment or may have leaked from a capillary used as a standard for the <sup>19</sup>F NMR spectra.

**Properties of ClCO<sup>+</sup>Sb<sub>3</sub>F<sub>16</sub><sup>–</sup>.** The ClCO<sup>+</sup>Sb<sub>3</sub>F<sub>16</sub><sup>–</sup> salt is a white solid which is thermally stable up to about –10 °C and decomposes to give ClFCO, SbF<sub>5</sub>, and some F<sub>2</sub>CO and SbF<sub>4</sub>Cl resulting from a chlorine–fluorine exchange between ClFCO and SbF<sub>5</sub>. This competing halogen exchange reaction prevented the determination of a reliable heat of dissociation from an Arrhenius plot of the vapor pressure–temperature data. The identity of the anion as *cis*-Sb<sub>3</sub>F<sub>16</sub><sup>–</sup><sup>18</sup> was established by its low-temperature <sup>19</sup>F NMR spectrum in SO<sub>2</sub>ClF solution (see Experimental Section). The ClCO<sup>+</sup> cation was identified by its <sup>13</sup>C NMR signal of 134 ppm<sup>8</sup> and vibrational spectroscopy (see below).

**Vibrational Spectra.** Infrared and Raman spectra are ideally suited to distinguish between ionic salts and covalent donor–acceptor adducts.<sup>35</sup> As can be seen from eq 7, the formation of



a halocarbonyl cation from the corresponding carbonyl dihalide results in a strengthening of both the C–O and the C–X bonds due to increased bond orders caused by electron back-donation from the ligands to the carbocation center, resulting in shifts to higher frequencies. In addition, the number of normal modes is

(30) Becke, A. D. *J. Chem. Phys.* **1993**, *98*, 5648.

(31) (a) Melius, C. F.; Goddard, W. A. *Phys. Rev. A* **1974**, *10*, 1528. (b) Kahn, L. R.; Baybutt, P.; Truhlar, D. G. *J. Chem. Phys.* **1976**, *65*, 3826. (c) Krauss, M.; Stevens, W. J. *Annu. Rev. Phys. Chem.* **1985**, *35*, 357. (d) Stevens, W. J.; Basch, H.; Krauss, M. *J. Chem. Phys.* **1984**, *81*, 6026. (e) Stevens, W. J.; Basch, H.; Krauss, M.; Jasien, P. *Can. J. Chem.* **1992**, *70*, 612. (f) Cundari, T. R.; Stevens, W. J. *J. Chem. Phys.* **1993**, *98*, 5555.

(32) The diffuse s+p function exponents used for Sb, Cl, F, O, and C were 0.0259, 0.0483, 0.1076, 0.0845, and 0.0438, respectively.

(33) The d function exponents used for Sb and Cl were 0.211 and 0.75, respectively. An exponent of 0.8 was used for F, O, and C.

(34) Dean, P. A. W.; Gillespie, R. J. *J. Am. Chem. Soc.* **1969**, *91*, 7260.

(35) Lindqvist, I. *Inorganic Adduct Molecules of Oxo-Compounds. Anorganische und Allgemeine Chemie in Einzeldarstellungen*; Becke-Goehring, M., Ed.; Academic Press Inc.: New York, 1963; Band IV.



reduced from 6 in  $X_2CO$  to three in  $XCO^+$ . On the other hand, for the O-coordinated, donor–acceptor adducts the bond order of the C–O bond is decreased, while that of the C–X bonds is increased. Furthermore, due to the additional bridge modes, the number of normal modes of the adduct is larger than the sum of the modes of the separate donor and acceptor molecules. The carbonyl stretching mode, which in ClFCO occurs at about  $1868\text{ cm}^{-1}$ ,<sup>36</sup> is well separated from the other modes and, therefore, is ideally suited to distinguish the  $CICO^+$  cation from an O-coordinated, donor–acceptor adduct.

The observed low-temperature infrared and Raman spectra of  $CICO^+$  in  $CICO^+Sb_3F_{16}^-$  are summarized in Table 1. As can be seen, the carbonyl stretching mode of  $CICO^+$  is shifted by  $+388\text{ cm}^{-1}$  relative to ClFCO,<sup>36</sup> and by  $+592\text{ cm}^{-1}$  relative to the ClFCO– $SbF_5$  donor–acceptor adduct, which has a carbonyl stretching frequency of  $1664\text{ cm}^{-1}$ .<sup>13</sup> This huge frequency increase firmly establishes the presence of the  $CICO^+$  cation. Of the remaining two normal modes of  $CICO^+$  (linear  $C_{\infty v}$   $CICO$  has two  $\Sigma$  stretching modes and one  $\pi$  bending mode), the C–Cl stretching mode was observed at  $803\text{ cm}^{-1}$ , whereas the bending mode is predicted by ab initio calculations (see below) and by comparison with the isoelectronic ClCN molecule<sup>37</sup> to fall within the range of the anion modes and to have very low Raman intensity and so it could not be located with confidence. Based on a private communication from Bernhardt, Willner and Aubke, who independently studied the vibrational spectra of  $CICO^+$ , the deformation mode is observed in the infrared spectrum at  $468\text{ cm}^{-1}$ .

Compared to ClFCO,<sup>36</sup> the C–Cl stretching frequency of  $CICO^+$  has also increased, as predicted above, although only by  $27\text{ cm}^{-1}$ . The dramatic difference between the frequency increases of the C–O and the C–Cl stretching modes demonstrates that the electron back-donation to the carbocation center in  $CICO^+$  involves mainly the oxygen atom and implies a dominant contribution from the  $[\overset{+}{X}-C\equiv O]$  resonance structure of eq 7. The triple bond character of the C–O bond in  $CICO^+$  is also supported by the fact that its C–O stretching frequency of  $2256\text{ cm}^{-1}$  is higher than that of CO ( $2143\text{ cm}^{-1}$ )<sup>38</sup> and that of the C–N bond in isoelectronic ClCN ( $2216\text{ cm}^{-1}$ ),<sup>37</sup> both of which undoubtedly possess well-defined triple bonds.

Further support for the presence of the  $CICO^+$  cation comes from the chlorine isotopic shift observed for the C–Cl stretching mode. Chlorine has two naturally occurring isotopes,  $^{35}\text{Cl}$  and  $^{37}\text{Cl}$ , with an abundance of 75.4 and 24.6%, respectively. The isotopic shift of about  $9\text{ cm}^{-1}$ , observed for  $\nu_3$  of  $CICO^+$  is in good agreement with the calculated value (see below) of  $9.9\text{ cm}^{-1}$  and that of  $8\text{ cm}^{-1}$  observed for the C–Cl stretching mode in isoelectronic ClCN.<sup>37</sup>

In addition to the two stretching modes of  $CICO^+$ , the combination band,  $(\nu_{CO} + \nu_{CCl})(\Sigma)$ , was also observed in the infrared spectrum at  $3056.1\text{ cm}^{-1}$  ( $2256 + 802.5 = 3058.5\text{ cm}^{-1}$ ). It exhibits a  $^{35}\text{Cl}$ – $^{37}\text{Cl}$  isotopic splitting of  $9.1\text{ cm}^{-1}$ , very similar to that observed for the C–Cl stretching mode, thereby clearly identifying this band as the combination band  $(\nu_1 + \nu_3)$  of  $CICO^+$  and confirming the assignment of the  $802.5\text{ cm}^{-1}$  band to the C–Cl stretching mode of  $CICO^+$ .

(36) Shimanouchi, T. *J. Phys. Chem. Ref. Data* **1977**, 6, 993 and references therein.

(37) Shimanouchi, T. Tables of Molecular Vibrational Frequencies, Consolidated Volume 1. NSRDS-NBS39. *Nat. Stand. Ref. Data Ser., Nat. Bur. Stand. (U.S.)* **1972** and references therein.

(38) Siebert, H. Anwendungen der Schwingungsspektroskopie in der Anorganischen Chemie. *Anorganische und Allgemeine Chemie in Einzeldarstellungen*; Becke-Goehring, M., Ed.; Springer-Verlag: Berlin, 1966; Band VII.

**Table 1.** Observed and Calculated Vibrational Spectra and Bond Lengths of  $CICO^+$  and Isoelectronic ClCN

assgnts and approx. mode descriptions in point group $C_{\infty v}$	obsd freq, $\text{cm}^{-1}$ (rel intens)			calcd freq, $\text{cm}^{-1}$ (IR int) [RA int] <sup>e</sup>					
	$CICO^+Sb_3F_{16}^-$		ClCN <sup>b</sup>	$CICO^+$		ClCN			
	IR	RA <sup>c</sup>	IR (gas)	RA (liq) <sup>c</sup>	RHF <sup>d</sup> $\omega$	CCSD(T) <sup>d</sup> $\omega$	CCSD(T)/cc-pVQZ <sup>e</sup> $\nu$	CCSD/cc-pVDZ <sup>e</sup> $\omega$	
$\nu_1(\Sigma)$ C $\equiv$ Y stretch ( $^{35}\text{Cl}$ )	2256 vs	2256(10)	2215.6 vs	2206(10)	2601.3 (505) [40.6]	2258(258)	2256.7	2220(19)	2242
C $\equiv$ Y stretch ( $^{37}\text{Cl}$ )			2215.3 vs		2601.1 (505) [40.6]				
$\nu_2(\pi)$ $^{35}\text{Cl}$ –C $\equiv$ Y bend	<i>e</i>	not obsd	378.4 s	394(3)	521.3 (27) [0]	472(21)	475.4	375(4)	382
$^{37}\text{Cl}$ –C $\equiv$ Y bend			378.0 s		520.7 (28) [0]				
$\nu_3(\Sigma)$ $^{35}\text{Cl}$ –C stretch	802.5 s	803(8)	744.2 f/s	730(5)	821.6 (33) [1.8]	773(28)	807.4	714(7)	
$^{37}\text{Cl}$ –C stretch	793.8 m	794(3)	736.0 s		811.8 (33) [1.8]				
$(\nu_1 + \nu_3)(\Sigma)$ $^{35}\text{Cl}$	3056.1 mw								
$^{37}\text{Cl}$	30470 w								
bond lengths									
$r(\text{C–Cl})$			1.6297 <sup>h</sup>		1.581	1.589	1.574	1.657	
$r(\text{C–X})$			1.1596		1.089	1.128	1.125	1.165	

<sup>a</sup> IR intensities in  $\text{km/mol}$ ; Raman intensities in  $\text{\AA}^4/\text{amu}$ . <sup>b</sup> Data from refs 37 and 43. <sup>c</sup> Uncorrected Raman intensities. <sup>d</sup> The 6-311+G(2d) basis set was used for these calculations. <sup>e</sup> Obscured by  $Sb_3F_{16}^-$  bands. <sup>f</sup> In the IR spectrum, this band is split by resonance with  $\nu_2$  into two intense bands at  $782.6$  and  $714.0\text{ cm}^{-1}$ . <sup>g</sup> Data from ref 39. <sup>h</sup> Data from ref 44.

The *cis*-Sb<sub>3</sub>F<sub>16</sub><sup>−</sup> anion, as expected for a 19 atom species, exhibits a very complex Raman spectrum (740 w, 717 m, 703 s, 693 m, 679 s, 670 m, 652 vs, 603 w, 336 vw, 300 mw, 274 mw, 260 sh, 235 w, 221 m). No attempts were made to assign this spectrum, since the identity of the anion is well established by the <sup>19</sup>F NMR spectra (see Experimental Section).

The F<sub>2</sub>CO/SbF<sub>5</sub> system was also studied by vibrational spectroscopy. The low-temperature reactions of F<sub>2</sub>CO with either excess SbF<sub>5</sub> in SO<sub>2</sub>ClF solution or solid SbF<sub>5</sub> matrixes did not generate any products exhibiting a high-frequency shift of the carbonyl stretching mode of F<sub>2</sub>CO (1928 cm<sup>−1</sup>),<sup>36</sup> and only the well-known F<sub>2</sub>CO·SbF<sub>5</sub> donor–acceptor adduct with  $\nu_{C-O} = 1770 \text{ cm}^{-1}$ <sup>10,13</sup> was observed. This lack of evidence for FCO<sup>+</sup> formation agrees well with results from the present NMR study.

**Theoretical Calculations.** High-level ab initio calculations have previously been reported for CICO<sup>+</sup>,<sup>39,40</sup> FCO<sup>+</sup>,<sup>7</sup> and isoelectronic CICN<sup>39</sup> and FCN,<sup>41,42</sup> the results of which were confirmed by the present work. Consequently, only the following six topics need to be discussed here.

**(i) Vibrational Frequencies and <sup>35</sup>Cl–<sup>37</sup>Cl Isotopic Shifts for CICO<sup>+</sup>.** Harmonic ( $\omega$ ) and anharmonic ( $\nu$ ) frequencies, together with observed<sup>37,42</sup> and calculated data for isoelectronic CICN, are summarized in Table 1. As can be seen, the CCSD-(T)<sup>39</sup> results are in excellent agreement with the observed spectra. The observed <sup>35</sup>Cl–<sup>37</sup>Cl isotopic shifts are also in accord with the calculations and clearly identify the vibrations involving a stretching of the C–Cl bond. The lower-level restricted Hartree–Fock calculations have also been included in Table 1 because they allowed the calculation of Raman intensities. As can be seen, the calculated Raman intensity of  $\nu_2$  of CICO<sup>+</sup> is vanishingly small, explaining the absence of  $\nu_2$  in our Raman spectrum.

Force fields for CICO<sup>+</sup> and CICN at the CCSD(T)/cc-pVQZ level with frequencies very close to those experimentally observed have previously been published.<sup>39</sup> The force constants of greatest interest,  $f(\text{CO}) = 19.663$  and  $f(\text{CCl}) = 6.455$  mdyne/Å,<sup>39</sup> are in accord with a strong CO triple bond ( $f(\text{CN})$  in CICN = 17.720 mdyne/Å and  $f(\text{CO})$  in CO = 18.56 mdyne/Å)<sup>37,38</sup> and a CCl bond with a bond order of 1.22, if the C–Cl bond in CICN ( $f = 5.290$  mdyne/Å)<sup>38</sup> is chosen as the basis for an sp-hybridized C–Cl single bond.

**(ii) Predicted Geometry for CICO<sup>+</sup>.** The excellent agreement of observed and calculated vibrational frequencies for CICO<sup>+</sup>, and comparison with the observed<sup>43,44</sup> and calculated structures for CICN (see Table 1), lend strong support to the previously proposed<sup>39</sup> geometry of  $r(\text{CO}) = 1.122 \text{ \AA}$  and  $r(\text{CCl}) = 1.567 \text{ \AA}$  for CICO<sup>+</sup>.

**(iii) NMR Shifts.** The calculated NMR chemical shifts of the isoelectronic CICO<sup>+</sup>/CICN and FCO<sup>+</sup>/FCN couples and CFCl<sub>3</sub> are summarized in Table 2 and compared to the experimentally observed shifts.<sup>8,45</sup> As can be seen, the agreement between the calculated and observed <sup>13</sup>C shifts of CICO<sup>+</sup> is good, thus lending further support to the verification of CICO<sup>+</sup>.

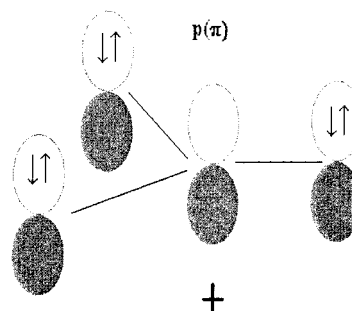
**Table 2.** Calculated and Observed NMR Shifts for the Isoelectronic Couples CICO<sup>+</sup>/CICN and FCO<sup>+</sup>/FCN and CFCl<sub>3</sub>

	calcd shifts <sup>a</sup>		obsd shifts	
	<sup>13</sup> C	<sup>19</sup> F	<sup>13</sup> C	<sup>19</sup> F
CICO <sup>+</sup>	134.5	–	133.7 <sup>b</sup>	–
CICN	94.0	–	94.7 <sup>c</sup>	–
FCO <sup>+</sup>	118.6	−70.5	[117.5] <sup>d</sup>	[not obsd] <sup>d</sup>
FCN	109.2	−128.2		−156.0 <sup>e</sup>
CFCl <sub>3</sub>		0	117.8 <sup>f</sup>	0

<sup>a</sup> MBPT(2)/6-311+G(2d) GIAO method. <sup>b</sup> Value from ref 8. <sup>c</sup> Value from ref 46. <sup>d</sup> Values attributed in ref 9a to FCO<sup>+</sup>. <sup>e</sup> Value from ref 45. <sup>f</sup> Value from this study.

**(iv) Stabilization of the Carbocation Centers in the XCO<sup>+</sup> Cations and Natural Bond Order Analyses.** The stability of carbocations is greatly enhanced by electron back-donation from a neighboring ligand, thus alleviating the electron deficiency of the carbenium center. This back-donation can occur either through the  $\sigma$  or p–p( $\pi$ ) bonds. If the ligand is more electronegative than C<sup>+</sup>, as is the case for fluorine, the  $\sigma$  back-donation becomes negative; i.e., the inductive effect of the fluorine ligand counteracts the p–p( $\pi$ ) back-donation. Consequently, the total ( $\sigma + \pi$ ) back-donation decreases with decreasing atomic weight of the halogen, i.e., I > Br > Cl > F. This point has recently been demonstrated by a natural bond order (NBO) analysis of the MX<sub>3</sub><sup>+</sup> and MH<sub>2</sub>X<sup>+</sup> series, where M = C, Si, Ge, Sn, Pb and X = F, Cl, Br, I.<sup>4</sup> It was, therefore, worthwhile to extend this NBO analysis to FCO<sup>+</sup> and CICO<sup>+</sup> and their isoelectronic counterparts in an effort to judge the relative contributions and the stabilizing or destabilizing effect of an oxygen ligand on the carbenium center. Calculations of atomic charge distributions can vary widely with the methods used, so they are not always reliable indicators of quantities such as bond orders or back-donation, which are not physically observable. Nevertheless, NBO analyses of similar compounds employing density matrixes calculated by the same methods should correctly reflect trends within the series. For more quantitative comparisons, bond distances or reliable force constants should be used, provided that they are corrected for secondary effects such as differences in the hybridization of the binding electrons.

In Frenking's NBO analysis<sup>4</sup> of CF<sub>3</sub><sup>+</sup>, the degree of p( $\pi$ ) back-donation from F to C was obtained by assuming the ideal carbenium resonance structure with an empty p( $\pi$ ) orbital



and the full positive charge being on carbon, while the three fluorines are  $\sigma$ -bonded through sp<sup>2</sup> hybridization. The p( $\pi$ ) back-donation from C to F was obtained by calculating for the minimum energy structure the actual p( $\pi$ ) population on carbon and dividing it by three to obtain the p( $\pi$ ) back-donation from each fluorine ligand. From this value and the calculated atomic charge distribution, the  $\sigma$  donation can be calculated according to eq 8.

(39) Pak, Y.; Woods, R. C. *J. Chem. Phys.* **1997**, *107*, 5094.

(40) Peterson, K. A.; Mayrhofer, R. C.; Woods, R. C. *J. Chem. Phys.* **1991**, *94*, 431.

(41) Lee, T. J.; Racine, S. C. *Mol. Phys.* **1995**, *84*, 717.

(42) Lee, T. J.; Martin, J. M. L.; Dateo, C. E.; Taylor, P. R. *J. Phys. Chem.* **1995**, *99*, 15858.

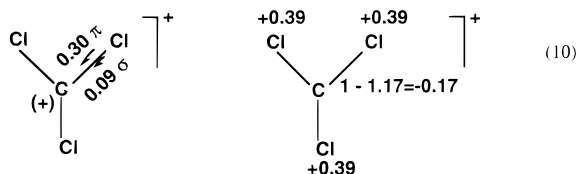
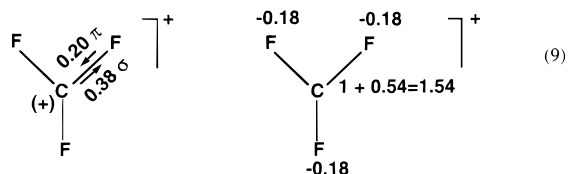
(43) Lafferty, W. J.; Lide, D. R.; Toth, R. A. *J. Chem. Phys.* **1965**, *43*, 2063.

(44) Saouli, A.; Dubois, I.; Blavier, J. F.; Bredohl, H.; Blanquet, G.; Meyer, C.; Meyer, F. *J. Mol. Spectrosc.* **1994**, *165*, 349.

(45) Fawcett, F. S.; Lipscomb, R. D. *J. Am. Chem. Soc.* **1960**, *82*, 1509; **1964**, *86*, 2576.

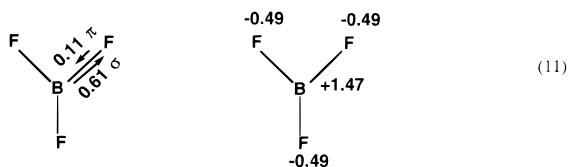
$$\text{atomic charge} = p(\pi) - \sigma \quad (8)$$

The results can best be summarized using simple arrow diagrams in combination with charge distributions, as shown in eqs 9 and 10 for  $\text{CF}_3^+$  and  $\text{CCl}_3^+$ , respectively.



Since  $\text{CF}_3^+$  and  $\text{CCl}_3^+$  are singly charged cations, the sum of their atomic charge distributions must equal +1. As can be seen from eqs 9 and 10, the  $p(\pi)$  back-donation increases from fluorine to chlorine, but the most dramatic effect is caused by the large change and sign reversal of the  $\sigma$  donation, which is caused by fluorine being more and chlorine being less electronegative than  $\text{C}^+$ . This strong negative  $\sigma$  effect of fluorine also preempts fluorine from acquiring a positive atomic charge, as might be implied from the simple fluoronium valence bond description  $(^+)\text{F}=\text{C}=\text{O}$ .

Extension of this NBO analysis to isoelectronic  $\text{BF}_3$  (eq 11) furthermore demonstrates that  $p(\pi)$  back-donation in  $\text{BF}_3$  is even

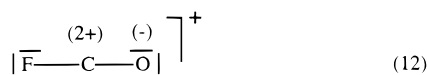


smaller than in  $\text{CF}_3^+$ . In view of the high stability of  $\text{BF}_3$ , insufficient  $p(\pi)$  back-donation in  $\text{CF}_3^+$  cannot be blamed for the elusiveness of  $\text{CF}_3^+$  in the condensed phase.

Extension of the NBO analyses to the halocarbonyl cations causes complications, because their two ligands are different and the second and third bonds of the carbonyl group are  $\pi$ -bonds. The following general approach successfully overcomes these complications: (i) all  $sp_n$  orbitals, which are required for the  $\sigma$ -bonded backbone, must be kept occupied, while all  $p(\pi)$  orbitals on the carbon central atom must be vacated and their electrons transferred to the ligands; (ii) the  $p(\pi)$  back-donation from each ligand is calculated by subtracting its actual  $p(\pi)$  orbital population from its fully occupied population value; and (iii) the  $\sigma$  donation from the central atom to the ligand is calculated by subtracting the atomic charge from the  $p(\pi)$  back-donation, under consideration of the formal charges generated by vacating the  $p(\pi)$  orbitals on the central atom.

The  $\text{FCO}^+$  cation is used to exemplify this approach.

Step i: All  $p(\pi)$  orbitals on carbon are vacated, and their electrons are transferred to the ligands, which generates the electron distributions and formal charges shown in eq 12.



Step ii: The following  $p(\pi)$  orbital populations were obtained from the ab initio calculations:

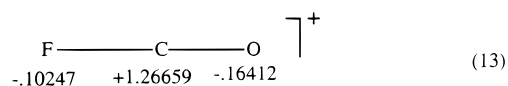
F:	$p_x$	1.84883	} 3.69766
	$p_y$	1.84883	
C:	$p_x$	0.68429	} 1.36858
	$p_y$	0.68429	
O:	$p_x$	1.43242	} 2.86484
	$p_y$	1.43242	
$\Sigma p_x + p_y =$			7.93108

Due to a small percentage of the electrons occupying higher orbitals or Rydberg states, the above sum of 7.93 electrons in the  $p_x$  and  $p_y$  orbitals is only 99.14% of the possible 8.0. Consequently, the fully occupied  $(p_x + p_y)\pi$  orbital population values on fluorine and oxygen in eq 12 must be normalized by 0.9914, giving  $4 \times 0.9914 = 3.96554$  electrons. The third free valence electron pairs on fluorine and oxygen can be ignored because they are  $p_z-\sigma$  pairs which cannot participate in the  $\pi$ -bonding. Subtraction of the above calculated  $(p_x + p_y)$  orbital population from the fully populated orbitals results in the following  $p(\pi)$  back-donation values:

$$\text{F: } 3.96554 - 3.69766 = 0.26788 \text{ electrons}$$

$$\text{O: } 3.96554 - 2.86484 = 1.10070 \text{ electrons}$$

Step iii: The calculated atomic charge distributions in  $\text{FCO}^+$  are

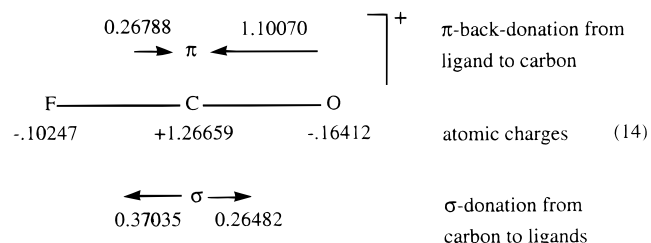


Subtraction of the atomic charge values from the sum of the formal charges on the specific ligands in eq 12 and the  $p(\pi)$  back-donation values obtained in step ii results in the following  $\sigma$  donation from carbon to the ligands:

$$\text{F: } 0.26788 + 0.10247 = 0.37035 \text{ electrons}$$

$$\text{O: } -1.00000 + 1.10070 + 0.16412 = 0.26482 \text{ electrons}$$

Using a simple arrow diagram to better visualize the  $\pi$ - and  $\sigma$ -donation effects and the resulting atomic charges, eq 13 can be rewritten in the following manner (eq 14), where the lengths of the arrows reflect the directions and magnitudes of the values:



The veracity of the above procedure can easily be crosschecked by starting with the formal charges on each atom in eq 12 and correcting them for the  $\sigma$  donations and  $p(\pi)$  back-donations; the result must equal the calculated atomic charges.

The results of our QCISD/6-311+G(2d) NBO analyses for  $\text{FCO}^+$ ,  $\text{ClCO}^+$ , and their isoelectronic counterparts  $\text{FCN}$  and  $\text{ClCN}$  are summarized in Table 3. They show that chlorine is a better  $p(\pi)$  back-donor than fluorine, and oxygen is a much



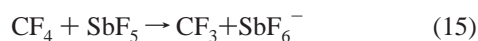
**Table 3.** Results from the NBO Analyses at the QCISD/6-311+G(2d) Level for FCO<sup>+</sup>, ClCO<sup>+</sup>, FCN, and ClCN<sup>a</sup>

$\begin{array}{c} 0.26788 \quad 1.10070 \\ \rightarrow \pi \leftarrow \\ (2+) \quad (-) \\ \left  \bar{F} - C - O \right  \\ \leftarrow \sigma \rightarrow \\ 0.37035 \quad 0.26482 \end{array} \quad \left. \begin{array}{c} + \\ + \end{array} \right\}$	$\begin{array}{c} -0.10247 \quad +1.26659 \quad -0.16412 \\ F - C \equiv O \\ 1.204 \quad 1.117 \end{array} \quad \left. \begin{array}{c} + \\ + \end{array} \right\}$
$\begin{array}{c} 0.39012 \quad 1.10260 \\ \rightarrow \pi \leftarrow \\ (2+) \quad (-) \\ \left  \bar{Cl} - C - O \right  \\ \leftarrow \sigma \rightarrow \\ 0.04807 \quad 0.27129 \end{array} \quad \left. \begin{array}{c} + \\ + \end{array} \right\}$	$\begin{array}{c} +.43819 \quad +.73050 \quad -0.16869 \\ Cl - C \equiv O \\ 1.590 \quad 1.122 \end{array} \quad \left. \begin{array}{c} + \\ + \end{array} \right\}$
$\begin{array}{c} 0.14438 \quad 1.68940 \\ \rightarrow \pi \leftarrow \\ (2+) \quad (2-) \\ \left  \bar{F} - C - N \right  \\ \leftarrow \sigma \rightarrow \\ 0.40532 \quad .09022 \end{array} \quad \left. \begin{array}{c} + \\ + \end{array} \right\}$	$\begin{array}{c} -0.26104 \quad +0.66186 \quad -0.40082 \\ F - C \equiv N \\ 1.271 \quad 1.156 \end{array} \quad \left. \begin{array}{c} + \\ + \end{array} \right\}$
$\begin{array}{c} 0.18198 \quad 1.76626 \\ \rightarrow \pi \leftarrow \\ (2+) \quad (2-) \\ \left  \bar{Cl} - C - N \right  \\ \leftarrow \sigma \rightarrow \\ 0.03799 \quad .07789 \end{array} \quad \left. \begin{array}{c} + \\ + \end{array} \right\}$	$\begin{array}{c} +0.14399 \quad +0.16765 \quad -0.31163 \\ Cl - C \equiv N \\ 1.656 \quad 1.158 \end{array} \quad \left. \begin{array}{c} + \\ + \end{array} \right\}$

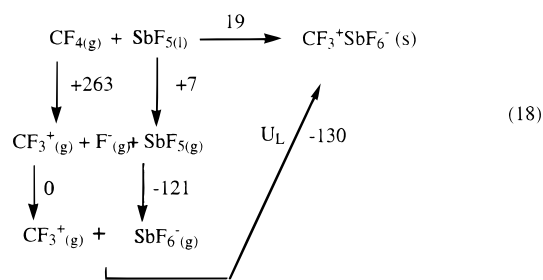
<sup>a</sup> The left column shows the p( $\pi$ ) back-donation from the ligands to the carbon atom, the  $\sigma$  donation from carbon to the ligands, and the formal charges generated by vacating all p( $\pi$ ) orbitals on carbon; the right column gives the atomic charges and calculated bond distances.

better p( $\pi$ ) back-donor than the halogens. This results in full triple bonds for the C–O and C–N bonds, but does not generate a positive atomic charge on oxygen, as the simple valence bond description,  $|\bar{F}-C\equiv O^{(+)}|$ , would require, thus demonstrating the pitfalls of atomic charges derived solely from valence bond descriptions. Table 3 also shows that the C $\equiv$ O bonds in FCO<sup>+</sup> and ClCO<sup>+</sup> are very similar. A comparison of the p( $\pi$ ) back-bonding from the halogens to carbon in CCl<sub>3</sub><sup>+</sup> (9) and ClCO<sup>+</sup> (Table 3), which exist in the condensed phase, and CF<sub>3</sub><sup>+</sup> (10) and FCO<sup>+</sup> (Table 3), which do not, does not show a significant difference, suggesting that a lack of p( $\pi$ ) back-bonding is not responsible for the elusiveness of CF<sub>3</sub><sup>+</sup> and FCO<sup>+</sup> in the condensed phase.

**(v) Thermodynamic Considerations.** The conclusion that a lack of p( $\pi$ ) back-bonding is probably not responsible for the elusiveness of CF<sub>3</sub><sup>+</sup> and FCO<sup>+</sup> in the condensed phase prompted us to scrutinize the overall thermodynamic aspects of reactions 15–17.



The reaction enthalpy of eq 15 can be estimated from the Born–Haber cycle (eq 18) to be endothermic by about 20 kcal/mol, using the JANAF values<sup>47</sup> for the ionization energy of CF<sub>4</sub>, a previously published estimate<sup>48</sup> for the heat of depolymerization and evaporation of liquid SbF<sub>5</sub>, a calculated value for the



fluoride affinity of SbF<sub>5</sub>,<sup>49</sup> and previously published methods<sup>50,51</sup> for estimating the lattice energy of CF<sub>3</sub><sup>+</sup>SbF<sub>6</sub><sup>−</sup>. Even if this latter number should be in error by as much as 20 kcal, it implies that the formation of CF<sub>3</sub><sup>+</sup>SbF<sub>6</sub><sup>−</sup> from CF<sub>4</sub> and SbF<sub>5</sub> is thermodynamically unfavorable. Therefore, the problem of preparing condensed state CF<sub>3</sub><sup>+</sup> salts is attributed to a combination of unfavorable overall thermodynamics (endothermicity of reaction 15 and high activation energy for breaking of the very strong C–F bond in CF<sub>4</sub>) and the lack of stable alternate starting materials, such as difluorocarbene, which could be oxidatively fluorinated with compounds such as XeF<sup>+</sup> or N<sub>2</sub>F<sup>+</sup>. For a successful CF<sub>3</sub><sup>+</sup> salt synthesis a Lewis acid will be required whose F<sup>−</sup> affinity exceeds that of SbF<sub>5</sub> by at least 20–30 kcal/mol. This estimate is based on the sum of the 19 kcal/mol endothermicity of eq 18 and the extrapolated 11 kcal/mol exothermicity of the competing formation of the oxygen-bridged, F<sub>2</sub>CO $\cdots$ SbF<sub>5</sub>, donor–acceptor complex.<sup>13</sup> Since SbF<sub>5</sub> has the highest known fluoride ion affinity,<sup>49</sup> it appears unlikely that a substantially stronger Lewis acid can be found.

Analogous Born–Haber cycles for eqs 16 and 17 give estimates of about 4 and −12 kcal/mol, respectively. Considering that the dissociation enthalpies of oxygen bridged donor–acceptor adducts, such as ClFCO $\cdots$ SbF<sub>5</sub>, are about 10–15 kcal/mol for SbF<sub>5</sub> adducts and 15–25 kcal/mol for AsF<sub>5</sub> adducts, it is then not surprising that the oxygen bridged donor–acceptor adducts are favored over the ionic adducts. Even for ClFCO, the use of a single SbF<sub>5</sub> molecule is still insufficient to produce ClCO<sup>+</sup>SbF<sub>6</sub><sup>−</sup>, and at least three SbF<sub>5</sub> molecules must be used to form ClCO<sup>+</sup>Sb<sub>3</sub>F<sub>16</sub><sup>−</sup> by increasing the F<sup>−</sup> affinity of the Lewis acid and by decreasing the depolymerization enthalpy<sup>48</sup> of liquid SbF<sub>5</sub>. Apparently, these effects outweigh the decrease in lattice energy, expected for the increased molecular volume.<sup>50</sup> The same arguments hold for the Cl<sub>2</sub>CO/SbF<sub>5</sub> system, where an analogous Born–Haber cycle estimate shows the formation of the oxygen bridged donor–acceptor adduct to be favored by about 10 kcal/mol over that of the ionic ClCO<sup>+</sup>SbF<sub>5</sub>Cl<sup>−</sup> salt.

**(vi) Theoretical Evaluations of the SbF<sub>5</sub> + ClFCO and Sb<sub>3</sub>F<sub>15</sub> + ClFCO Systems.** The interaction of ClFCO with a strong Lewis acid, such as SbF<sub>5</sub>, represents the very interesting case of a donor molecule possessing three competing donor sites, i.e., oxygen, fluorine, and chlorine. In the case of an attractive halogen interaction, a complete transfer of one halogen to the Lewis acid under formation of a halocarbonyl cation and an SbF<sub>5</sub>X<sup>−</sup> anion could occur. Further interest stems from the observation that SbF<sub>5</sub> forms with ClFCO only an oxygen-bridged donor–acceptor adduct, whereas Sb<sub>3</sub>F<sub>15</sub> forms an ionic ClCO<sup>+</sup>Sb<sub>3</sub>F<sub>16</sub><sup>−</sup> salt. It was, therefore, desirable to investigate whether such a complex system could be modeled and predicted correctly by theoretical methods.

(46) Walker, N.; Fox, W. B.; De Marco, R. A.; Moniz, W. B. *J. Magn. Reson.* **1977**, *27*, 345.

(47) *JANAF Interim Thermochemical Tables*; The Dow Chemical Co.: Midland, MI, 1965 and subsequent revisions.

(48) Bougon, R.; Bui Huy, T.; Burgess, J.; Christe, K. O.; Peacock, R. D. *J. Fluor. Chem.* **1982**, *19*, 263.

(49) Dixon, D. A.; Christe, K. O. Unpublished results.

(50) Richardson, T. J.; Tanzella, F. L.; Bartlett, N. *J. Am. Chem. Soc.* **1986**, *108*, 4937.

(51) Petrie, M. A.; Sheehy, J. A.; Boatz, J. A.; Rasul, G.; Prakash, G. K. S.; Olah, G. A.; Christe, K. O. *J. Am. Chem. Soc.* **1997**, *119*, 8802.

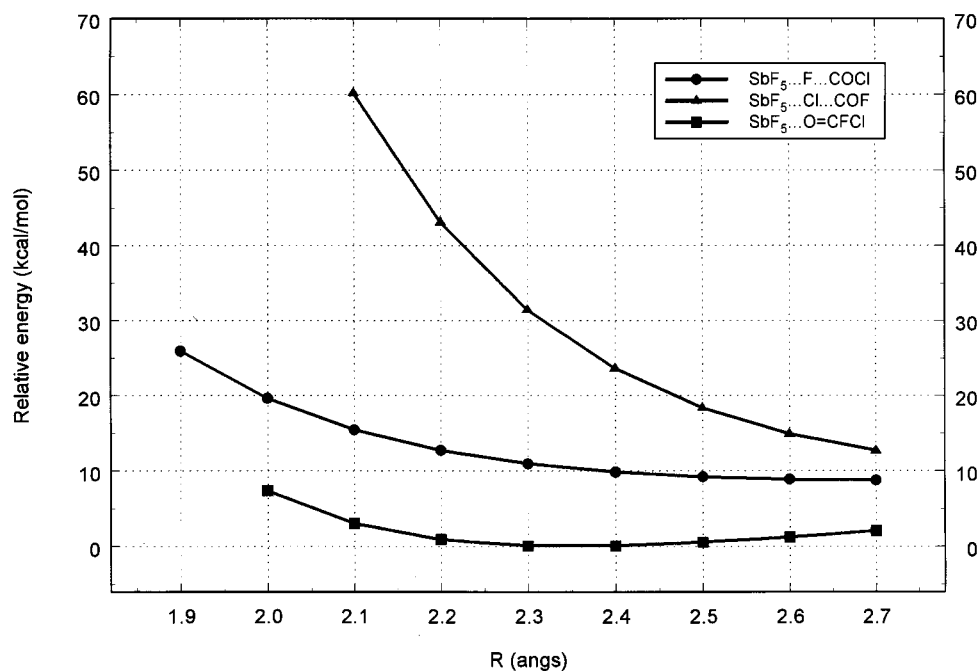


**Figure 1.** B3LYP/SBK+(d) energies of partially optimized geometries for fluorine-, chlorine-, and oxygen-bridged interactions of ClFCO and SbF<sub>5</sub>. The Sb–F (circles, Sb–Cl (triangles), and Sb–O (squares) internuclear distances were held fixed at the indicated *R* values, with the remaining geometrical degrees of freedom fully optimized. Energies (in kcal/mol) are relative to the fully optimized SbF<sub>5</sub>···O=CFCI local minimum.

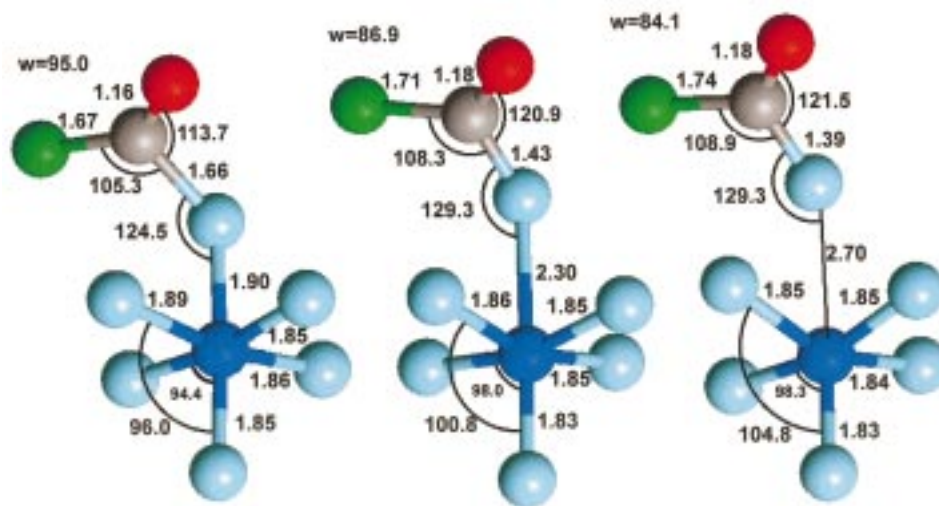


**Figure 2.** B3LYP/SBK+(d) partially optimized geometries (bond lengths in Å, bond angles in degrees) for three points on the potential energy curve of Figure 1 for the fluorine-bridged approach of SbF<sub>5</sub> by ClFCO. The distance between the Sb atom and the F atom on ClFCO was held fixed at values of 1.9, 2.3, and 2.7 Å, with the remaining structural degrees of freedom fully optimized. The dihedral angle “W” is defined as the angle that the ClCO plane forms with respect to the SbFC plane. Color code: green = Cl, red = O, gray = C, light blue = F, dark blue = Sb.

In view of the relatively large size of the molecules involved, density functional methods and effective core potentials (B3LYP/SBK+(d)) were used for our calculations.<sup>30–33</sup> For the SbF<sub>5</sub>/ClFCO system a sequence of constrained optimizations were performed in which the distance between the Sb atom and the F atom on ClFCO was held fixed while the remaining geometrical degrees of freedom were fully optimized. Similar calculations were also carried out in which the Sb–Cl and Sb–O distances were likewise fixed. The energy profiles as a function of the fixed Sb–F, Sb–Cl, and Sb–O distances are shown in Figure 1, and selected optimized geometries for each approach are shown in Figures 2–4. Figure 1 indicates that the potential energy curves for chlorine- and fluorine-bridging are repulsive and do not show a minimum, with the chlorine curve being

more repulsive than that for fluorine. Furthermore, the carbonyl halide groups in the fluorine- and chlorine-bridged structures do not lie in the paper planes of Figures 2 and 3, but form dihedral angles ranging from about 80 to 130° with respect to the paper planes, resulting in *C*<sub>1</sub> symmetry. The corresponding *C*<sub>s</sub> symmetry structures, in which the carbonyl halide ligands lie in the paper planes of Figures 2 and 3 are about 1 kcal/mol higher in energy.

For the oxygen-bridged ClFCO·SbF<sub>5</sub> adduct, Figure 1 shows a shallow minimum, in agreement with the experimental finding of a weak donor–acceptor adduct. In this adduct, the two halogen ligands of the ClFCO group lie in the paper planes of Figure 4, resulting in *C*<sub>s</sub> symmetry. The structure in which the fluorine ligand of ClFCO points toward the SbF<sub>5</sub> group (Figure



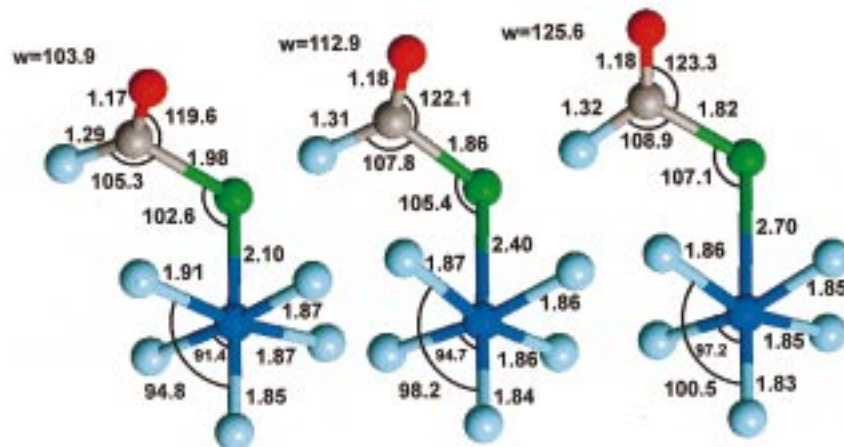


**Figure 3.** B3LYP/SBK+(d) partially optimized geometries (bond lengths in Å, bond angles in degrees) for three points on the potential energy curve of Figure 1 for the chlorine-bridged approach of  $\text{SbF}_5$  by ClFCO. The distance between the Sb atom and the Cl atom on ClFCO was held fixed at values of 2.1, 2.4, and 2.7 Å, with the remaining structural degrees of freedom fully optimized. The dihedral angle "W" is defined as the angle that the FCO plane forms with respect to the SbClC plane. Color code: green = Cl, red = O, gray = C, light blue = F, dark blue = Sb.

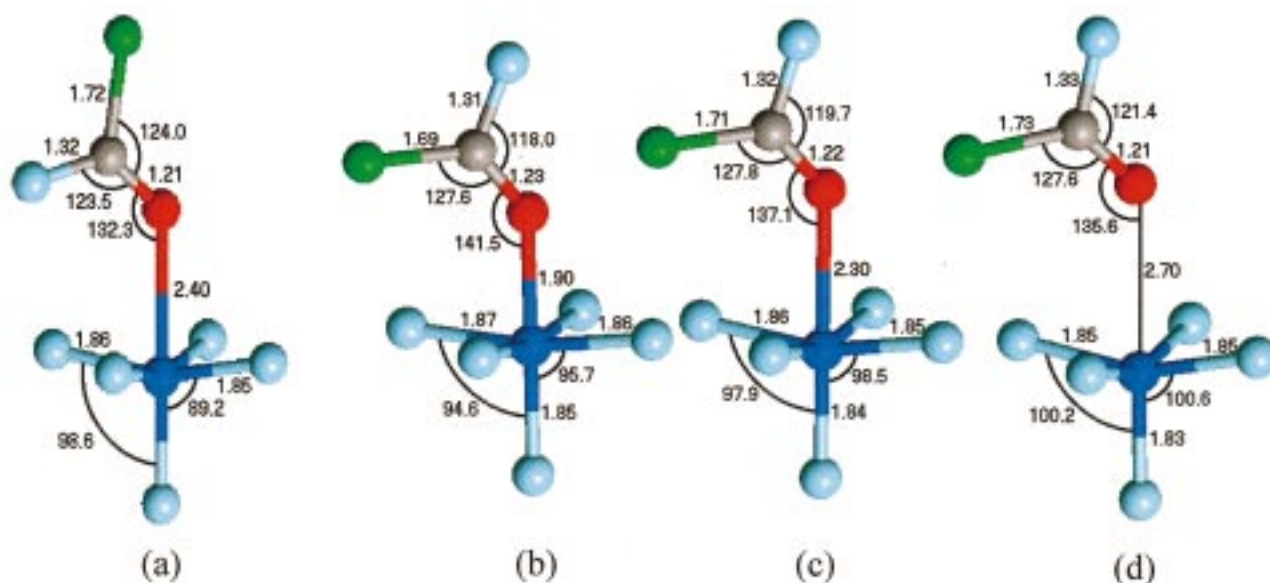


**Figure 4.** B3LYP/SBK+(d) partially optimized geometries (bond lengths in Å, bond angles in degrees) for the oxygen-bridged approach of  $\text{SbF}_5$  by ClFCO. Structure a, in which the chlorine atom points away from the  $\text{SbF}_5$  adduct, has a fixed Sb–O distance of 2.4 Å but is otherwise fully optimized. Structures b–d likewise are partially optimized geometries for three points on the potential energy curve of Figure 1, in which the Sb–O distance is held fixed at 1.9, 2.3, and 2.7 Å, respectively. Color code: green = Cl, red = O, gray = C, light blue = F, dark blue = Sb.

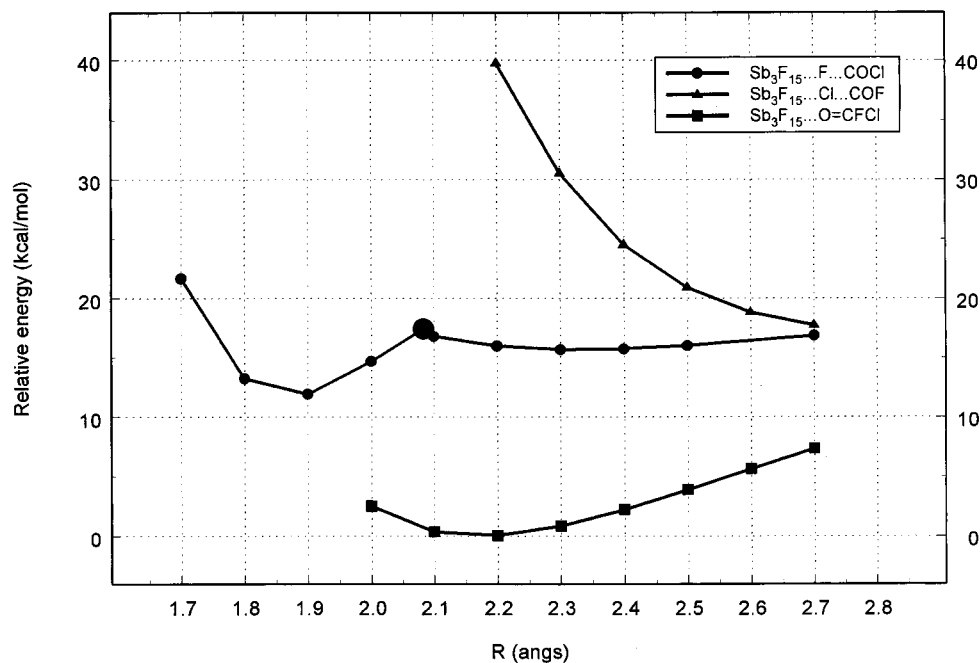
4a) is only slightly lower (by 0.03 kcal/mol for  $R(\text{Sb}-\text{O}) = 2.4$  Å) in energy than the corresponding structure in which the chlorine ligand points toward  $\text{SbF}_5$ , and their geometries are very similar.

Analogous calculations were also done for the  $\text{Sb}_3\text{F}_{15} + \text{ClFCO}$  system, in which the distance between the central Sb atom in  $\text{Sb}_3\text{F}_{15}$  and the F, Cl, or O atom of ClFCO was held fixed, with the resulting energy curves shown in Figure 5. The chlorine-bridged approach was again repulsive, and a typical geometry for one of the points on the curve is shown in two different perspectives in Figure 6a. Other configurations, with the fluorine ligand of ClFCO pointing up or the COClF group being rotated by  $180^\circ$ , i.e., pointing away from the  $\text{Sb}_3\text{F}_{15}$  group, were found to be higher in energy by 1.67 and 3.6 kcal/mol, respectively, for  $R(\text{Sb}-\text{Cl}) = 2.30$  Å.

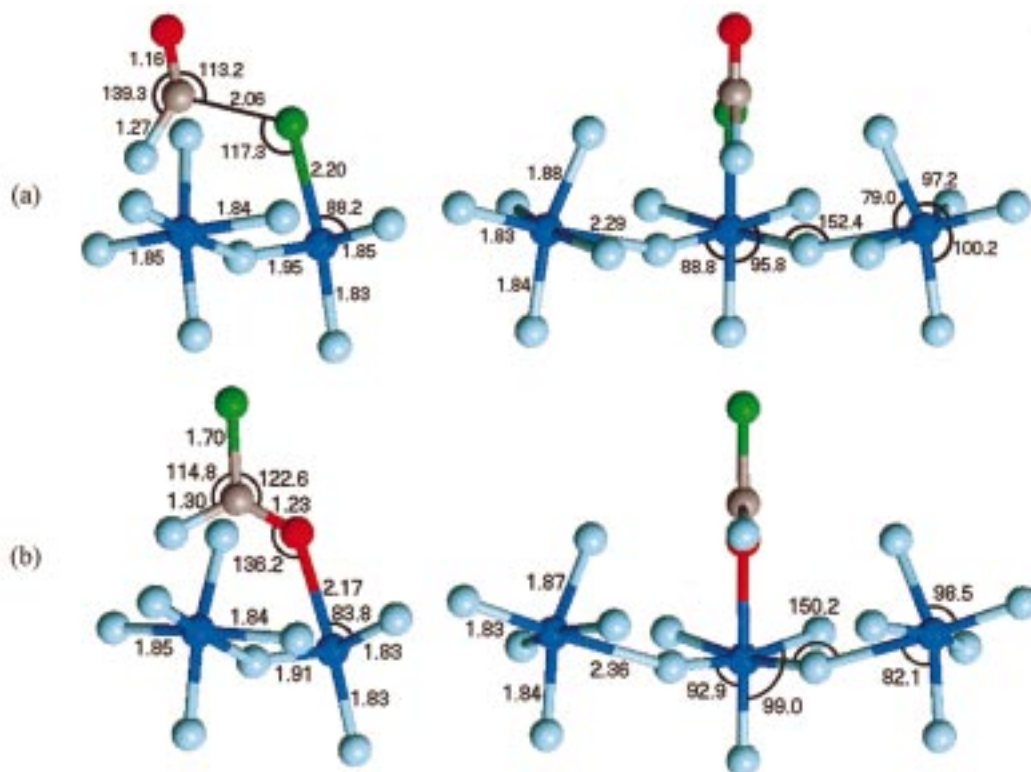
For the oxygen-bridged approach of  $\text{Sb}_3\text{F}_{15}$  by ClFCO a shallow minimum was found for its potential energy curve (see

Figure 5), indicative of a marginally stable donor–acceptor adduct. Figure 6b shows two perspectives of its fully optimized minimum energy geometry. As can be seen, this adduct has  $C_s$  symmetry. Other conformations (with the fluorine ligand of ClFCO pointing up and/or with the ClFCO ligand rotated by  $180^\circ$ ) were explored, but found to be higher in energy by about 1–2 kcal/mol.

The fluorine-bridged approach of  $\text{Sb}_3\text{F}_{15}$  by ClFCO results in a well-defined minimum, corresponding to the transfer of a fluoride ion from ClFCO to  $\text{Sb}_3\text{F}_{15}$  with formation of the ionic salt  $\text{ClCO}^+ \text{Sb}_3\text{F}_{16}^-$  (see Figure 7). The transition state for the fluoride ion transfer, represented by the large circle in Figure 5, occurs at an  $R(\text{Sb}-\text{F})$  distance of 2.08 Å and is shown in the middle structure of Figure 7. The magnitude of the single imaginary harmonic frequency is  $111 \text{ cm}^{-1}$ , and the corresponding vibrational mode's displacement vectors (not shown) clearly indicate simultaneous cleavage of the C–F bond and the



**Figure 5.** B3LYP/SBK+(d) energies of partially optimized geometries for fluorine-, chlorine-, and oxygen-bridged interactions of ClFCO and  $\text{Sb}_3\text{F}_{15}$ . The Sb–F (circles), Sb–Cl (triangles), and Sb–O (squares) internuclear distances were held fixed at the indicated  $R$  values, with the remaining geometrical degrees of freedom fully optimized. Energies (in kcal/mol) are relative to the fully optimized  $\text{Sb}_3\text{F}_{15}\cdots\text{O}=\text{CFCI}$  local minimum. The transition state for the  $\text{Sb}_3\text{F}_{15} + \text{ClFCO} \rightarrow [\text{Sb}_3\text{F}_{16}]^- [\text{COCl}]^+$  fluoride anion transfer reaction is indicated by the large circle. Color code: green = Cl, red = O, gray = C, light blue = F, dark blue = Sb.



**Figure 6.** (a) Two perspectives of the B3LYP/SBK+(d) chlorine-bridged constrained geometry in which the Sb–Cl distance is fixed at 2.2 Å. (b) Two perspectives of the B3LYP/SBK+(d) oxygen-bridged fully optimized geometry. Color code: green = Cl, red = O, gray = C, light blue = F, dark blue = Sb.

formation of an Sb–F bond. Although the minimum for the oxygen-bridged ClFCO· $\text{Sb}_3\text{F}_{15}$  adduct is about 12 kcal/mol lower than that for the ionic  $\text{ClCO}^+\text{Sb}_3\text{F}_{16}^-$  ion pair, it must be kept in mind that these potentials are for the free gaseous species. In the condensed phase, the larger lattice energy of the

ionic form lowers its energy well below that of the oxygen-bridged donor–acceptor adduct and confirms the experimental finding of the ionic salt.

These computations demonstrate that it is possible to predict correctly not only the preferred coordination site, i.e., oxygen

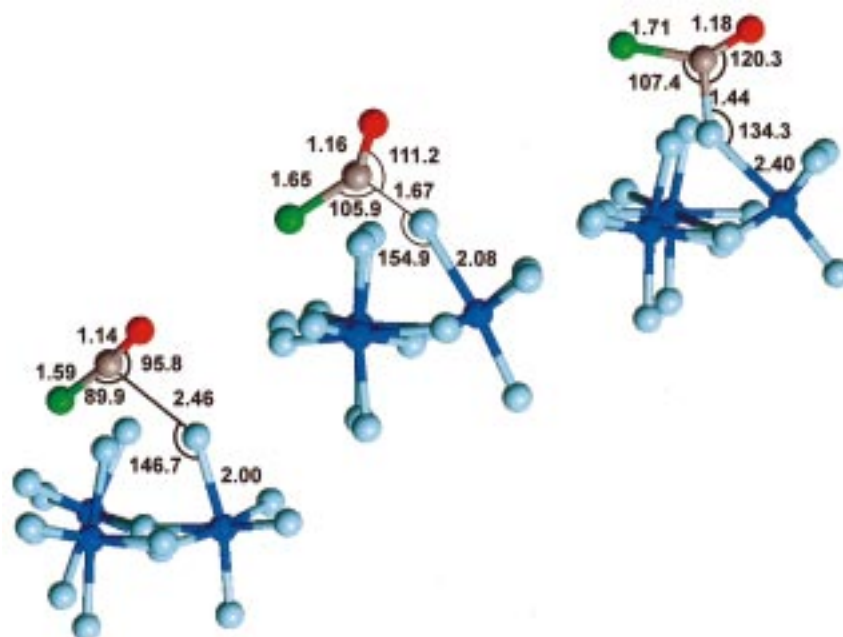


**Figure 7.** B3LYP/SBK+(d) geometries (bond lengths in Å, bond angles in degrees) for three points on the potential energy curve of Figure 5 for the fluorine-bridged approach of  $\text{Sb}_3\text{F}_{15}$  by ClFCO. The distance between the Sb atom and the F atom on ClFCO was held fixed at values of 2.0 and 2.4 Å in the lower left and upper right structures, respectively. The middle structure is the fully optimized transition state for the fluoride anion transfer reaction. Color code: green = Cl, red = O, gray = C, light blue = F, dark blue = Sb.

versus fluorine versus chlorine, but also whether a covalent oxygen-bridged, donor–acceptor complex is favored over an ionic complex, which can emanate from a halogen-bridge. Our calculations also correctly predict that  $\text{SbF}_5$  is not sufficiently acidic to remove a fluoride ion from ClFCO, but  $\text{Sb}_3\text{F}_{15}$  can do so. Furthermore, they confirm the conclusions and rough energy estimates derived from the Born–Haber cycles.

### Conclusions

Our experimental and computational studies show that with the presently known Lewis acids the synthesis of condensed phase  $\text{CF}_3^+$  salts cannot be achieved due to unfavorable overall thermodynamics. For  $\text{FCO}^+$  salts, the situation becomes somewhat more favorable, but the formation of covalent, oxygen-bridged, donor–acceptor complexes between  $\text{F}_2\text{CO}$  and the Lewis acids is still clearly favored, and the previous report of the observation of  $\text{FCO}^+$  in solution by NMR spectroscopy could not be confirmed. For ClFCO, the formation of either  $\text{CICO}^+$  salts or oxygen-bridged, ClFCO·Lewis acid, donor–acceptor adducts was observed, depending on the strength of the Lewis acid used. Computational methods were used to

calculate the extent of  $\sigma$  donation and  $p(\pi)$  back-donation in compounds containing more than one type of ligand, and also for predicting either covalent adducts or ionic salts emanating from Lewis bases with three different coordination sites.

**Acknowledgment.** The authors thank Drs. S. L. Rodgers and P. G. Carrick for their active support. The work at the Air Force Research Laboratory was financially supported by the Propulsion Directorate and that at USC by the National Science Foundation. B.H. thanks the Deutsche Forschungsgemeinschaft for a stipend. This work was also supported in part by a grant of Cray T916 time from the Army Research Laboratory Department of Defense High Performance Computing Center. After completion of our study and presentation of our results at two meetings,<sup>12</sup> Drs. H. Willner and F. Aubke kindly provided us with the results from their unpublished study of the vibrational spectra of isotopically substituted  $\text{CICO}^+$ , which are in good agreement with our data. This paper is dedicated to Dr. Roland Bougon on the occasion of his 65th birthday.

IC990572O